antibiotics

MDPI

Article

Synergistic and Additive Antibacterial Activity of Biogenic Silver Nanoparticles Combined with *Scaptotrigona bipunctata* Honey Against Reference and Multidrug-Resistant Bacterial Pathogens

Matheus Alves Pauletti *, Marcelly Chue Gonçalves, Sara Scandorieiro, Leonardo Pinto Medeiros, Laura Pierobão, Anastácia Nikolaos Deonas, Renata Katsuko Takayama Kobayashi and Gerson Nakazato *

Laboratory of Basic and Applied Bacteriology, Department of Microbiology, Center of Biological Sciences, Universidade Estadual de Londrina, Londrina 86057-970, Brazil
* Correspondence: matheuspauletti839@gmail.com (M.A.P.); gnakazato@uel.br (G.N.)

Abstract

Background/Objectives: Resistance and toxicity limit topical agents for infected burns. We evaluated biogenic silver nanoparticles (bio-AgNPs) combined with Brazilian stingless bee *Scaptotrigona bipunctata* honey (SB honey). Methods: Bio-AgNPs and honeys from three stingless bee species and *Apis mellifera* were screened against 11 reference and multidrug-resistant (MDR) strains, including MRSA, MDR *Escherichia coli*, and MDR *Pseudomonas aeruginosa*. The most active, SB honey, was combined with bio-AgNPs and assessed by checkerboard (FICI), time-kill, and scanning electron microscopy (SEM). Each agent's cytotoxicity was determined in HaCaT keratinocytes. Results: Combinations were synergistic (FICI 0.50) against the three Gram-negative strains tested and additive (FICI 0.75) against the three Gram-positive ones, lowering both inhibitory concentrations up to fourfold. The combination reduced viable counts below detection faster than either agent alone at its MBC against MDR *P. aeruginosa* (30 vs. 60 min) and *S. aureus* (7 vs. 10–24 h), and matched the fastest single agent against *E. coli*, at two- to fourfold lower concentrations of both. SEM showed surface damage and incomplete septa. These reduced concentrations fell below each agent's CC_{50}, increasing the calculated selectivity index. Conclusions: Bio-AgNPs and SB honey act jointly against the reference and MDR strains tested, all associated with burn infections, at concentrations below each agent's cytotoxic threshold, supporting their further development as a topical antimicrobial.

Keywords: burn wound infection; drug combination; green synthesis; Meliponini; MRSA; nanotechnology; stingless bee honey; *Trichilia catigua*

Check for updates

Academic Editors: Piotr Szweda and Karolina Matejczuk

Received: 28 September 2026
Revised: 20 October 2026
Accepted: 21 October 2026
Published: 23 October 2026

Copyright: © 2026 by the authors. Licensee MDPI, Basel, Switzerland. This article is an open access article distributed under the terms and conditions of the Creative Commons Attribution (CC BY) license.

1. Introduction

Antimicrobial resistance poses an alarming and escalating threat to global public health, with projections estimating over 39 million deaths attributable to drug-resistant bacterial infections by 2050 [1]. This crisis is especially pronounced in burn patients, in whom the loss of the protective skin barrier and compromised immune responses create a favorable environment for opportunistic infections [2].

Multidrug-resistant (MDR) pathogens, particularly *Pseudomonas aeruginosa* and methicillin-resistant *Staphylococcus aureus* (MRSA), along with other Gram-negative organisms such as *Acinetobacter baumannii*, are prevalent in burn wound infections and

are associated with increased morbidity and mortality, further complicating therapeutic management [3,4].

Conventional treatments have often proven inadequate in the face of MDR infections [5], underscoring an urgent need for innovative antimicrobial strategies that can circumvent bacterial resistance mechanisms while remaining safe and effective for clinical application. Among emerging alternatives, silver nanoparticles (AgNPs) and bioactive natural products such as honey have attracted considerable attention due to their broad-spectrum antimicrobial activity. Importantly, honey has been reported to rarely select for stable resistance under repeated exposure [6,7], and certain native honeys, including those from Brazilian stingless bees, may possess unique bioactive profiles relevant to wound care [8,9].

Although AgNPs can exhibit toxicity at high concentrations, their antimicrobial efficacy can be enhanced when combined with other agents [10], allowing effective use at lower, less toxic doses. In this context, pairing AgNPs with honey, which is well tolerated by host tissue and exhibits minimal systemic toxicity [11], may reduce the concentration of each agent required for antibacterial activity, and, with it, the associated cytotoxicity.

The nanoparticles used here also differ in how they are produced. Beyond conventional chemical routes, AgNPs can be obtained by green (biogenic) synthesis, in which plant extracts serve simultaneously as reducing and capping agents, converting Ag^+ to metallic silver under mild conditions while stabilizing the resulting particles [12]. Unlike chemically synthesized particles stabilized by simple agents such as citrate or borohydride, biogenically produced AgNPs retain a surface layer of phytochemicals from the source extract [13]. This capping layer is not merely a stabilizer: the adsorbed biomolecules have been associated with the colloidal stability and biological activity of the particles and can influence how they interact with biological membranes [14]. In the present work, the bio-AgNPs were synthesized from a *Trichilia catigua* (catuaba) bark extract, so their surface carries phytochemicals derived from this plant rather than a synthetic stabilizer.

Beyond their antimicrobial properties, both honey and AgNPs have been reported to support wound healing, which adds to their interest for burn management. Honey's composition, rich in sugars, enzymes, antioxidants, and other bioactive compounds, has been associated with tissue regeneration, reduced inflammation, and angiogenesis [15,16], while AgNPs have been reported to modulate inflammatory responses and support fibroblast proliferation and migration, alongside recognized challenges regarding cytotoxicity and stability [17]. These complementary profiles further motivate testing the two agents in combination.

Honeybee honey has also been used in place of plant extracts for the green synthesis of AgNPs [18,19], an approach more recently extended to stingless bee honey [20,21] and pollen [22], and to microorganisms associated with stingless bee colonies [23]. In these studies, however, the bee product is consumed in synthesis and becomes part of the nanoparticle itself, rather than being used as a separate agent alongside it. Honey–silver nanoparticle combinations in which the two agents were tested separately have yielded mixed antibacterial outcomes, from synergy to indifference [24–26]; in all of them, the nanoparticles were chemically synthesized and the honey came from *Apis mellifera* or was of undeclared origin. Stingless bee honeys therefore remain largely unexplored as combination partners for AgNPs. This leaves a specific gap: whether two biologically derived agents, a phytochemical-capped biogenic nanoparticle and a Meliponini honey, behave differently in combination from their conventional counterparts. Both differ substantially from the nanoparticles and honeys used in those studies, and either difference could reshape the nature and magnitude of the interaction.

Accordingly, this work first screened the individual antibacterial activities of biogenic silver nanoparticles and four honeys (*Scaptotrigona bipunctata*, *Tetragona clavipes*, *Tetragonisca angustula*, and *Apis mellifera*) against a panel of reference and multidrug-resistant pathogens. Honey from *Scaptotrigona bipunctata*, the most active of the four, was then selected for detailed study in combination with the nanoparticles. Specifically, we evaluated the antibacterial interaction (checkerboard/FICI), killing kinetics (time-kill curves), effects on cell surface morphology (scanning electron microscopy) and cytotoxicity toward human keratinocytes (MTT assay), from which the selectivity index was derived, to establish, in vitro, whether this biologically derived combination is effective against resistant pathogens relevant to burn wounds.

2. Results

2.1. Honey pH and Baseline Antibacterial Screening of the Isolated Agents

All four honeys were characteristically acidic, with pH values across species corresponding to: *A. mellifera* (3.50 ± 0.10), *S. bipunctata* (3.45 ± 0.09), *T. angustula* (3.88 ± 0.12), and *T. clavipes* (4.10 ± 0.09).

The isolated antibacterial activities of the four honeys and the green-synthesized silver nanoparticles (bio-AgNPs) were initially screened across the complete bacterial panel. As detailed in Table 1, marked differences in susceptibility were observed between pathogen types and treatment agents.

Table 1. Minimum inhibitory concentration (MIC) and minimum bactericidal concentration (MBC) of honeys from *Apis mellifera*, *Scaptotrigona bipunctata*, *Tetragona clavipes*, and *Tetragonisca angustula*, and of biogenic silver nanoparticles (bio-AgNP), against reference and multidrug-resistant bacterial strains. In each cell, the first value refers to the MIC and the second to the MBC.

Bacterial Strain	*A. mellifera*	*S. bipunctata*	*T. clavipes*	*T. angustula*	Bio-AgNP
	% (*v*/*v*)	% (*v*/*v*)	% (*v*/*v*)	% (*v*/*v*)	µM
Gram-positive					
S. aureus ATCC 25923	20/20	1.25/2.5	5/10	5/10	62.5/125
S. aureus BMB9393 (MRSA)	>20/>20	1.25/2.5	5/10	5/10	62.5/125
S. pyogenes ATCC 19615	20/>20	1.25/5	10/10	10/10	62.5/250
S. epidermidis ATCC 12228	20/>20	1.25/1.25	10/20	10/20	31.25/125
C. acnes ATCC 6919	20/>20	2.5/2.5	10/10	5/10	250.0/500
Gram-negative					
E. coli ATCC 25922	20/20	5/10	10/10	10/10	62.5/125
E. coli 5616 (MDR)	>20/>20	5/10	10/20	10/20	125.0/250
P. aeruginosa ATCC 27853	20/20	5/10	10/10	5/10	15.62/31.25
P. aeruginosa 2491 (MDR)	20/>20	5/10	10/20	10/20	62.5/125
A. baumannii ATCC 19606	20/>20	2.5/2.5	5/10	10/20	31.25/62.5
K. pneumoniae ATCC 10031	>20/>20	5/10	10/10	20/20	31.25/62.5

ATCC—American Type Culture Collection; MRSA—methicillin-resistant *Staphylococcus aureus*; MDR—multidrug-resistant. Clinical isolates (BMB9393, 2491, 5616) are described in Section 4.1.

Traditional *Apis mellifera* honey exhibited limited overall efficacy, showing Minimum Inhibitory Concentrations (MICs) of 20% (*v*/*v*) against most reference strains, with no inhibition of MRSA BMB9393, MDR *E. coli* 5616 or *K. pneumoniae* ATCC 10031 at the highest concentration tested.

Conversely, native stingless bee honeys (Meliponini) demonstrated superior baseline potency. Among them, honey derived from *Scaptotrigona bipunctata* (SB honey) emerged as the most effective honey, displaying potent activity particularly against Gram-positive targets, with MIC values ranging from 1.25% to 2.5% (*v*/*v*). *Tetragona clavipes* and *Tetragonisca angustula* honeys followed, generally requiring higher inhibitory concentrations (5% to 20%

v/*v*). With the lowest MIC and MBC values across the whole panel, SB honey was selected for the subsequent combination assays.

The bio-AgNPs displayed their lowest MIC values against Gram-negative strains, most notably *Pseudomonas aeruginosa* ATCC 27853 (MIC 15.62 µM), followed by *Acinetobacter baumannii* ATCC 19606 and *Klebsiella pneumoniae* ATCC 10031 (MIC 31.25 µM each). Against Gram-positive reference strains, MIC values were generally higher, ranging from 31.25 µM (*Staphylococcus epidermidis* ATCC 12228) to 250 µM (*Cutibacterium acnes* ATCC 6919).

2.2. Synergistic and Additive Interaction Profiles

The combination of SB honey and bio-AgNPs was evaluated by checkerboard assay against six pathogens selected from the screening panel. Synergism (FICI $\leq$ 0.50) was observed against all three Gram-negative targets—*E. coli* ATCC 25922, *P. aeruginosa* ATCC 27853, and MDR *P. aeruginosa* 2491—with no indifferent or antagonistic interactions in any combination (Table 2). FICI values for each independent replicate, calculated relative to the MIC of each agent alone determined on the same plate, are given in Table S1. Under synergistic conditions, the MIC of SB honey was reduced fourfold (from 5.00% to 1.25% *v*/*v*), and the MIC of bio-AgNPs also decreased fourfold for all three strains.

Table 2. Checkerboard assay results for the combination of *Scaptotrigona bipunctata* (SB) honey and biogenic silver nanoparticles (bio-AgNP) against reference and multidrug-resistant bacterial strains, showing the minimum inhibitory concentrations (MIC) of each agent alone and in combination, the Fractional Inhibitory Concentration Index (FICI), and the resulting antibacterial interaction classification.

Bacteria	SB Honey % (*v*/*v*)		Bio-AgNP (µM)		FICI	Interaction
	MIC (i)	MIC (c)	MIC (i)	MIC (c)		
S. aureus ATCC 25923	1.25	0.62	62.50	15.62	0.75	Additive
MRSA BMB9393	1.25	0.62	62.50	15.62	0.75	Additive
S. epidermidis ATCC 12228	1.25	0.31	31.25	15.62	0.75	Additive
E. coli ATCC 25922	5.00	1.25	62.50	15.62	0.50	Synergistic
P. aeruginosa ATCC 27853	5.00	1.25	15.62	3.91	0.50	Synergistic
P. aeruginosa 2491	5.00	1.25	62.50	15.62	0.50	Synergistic

SB honey—honey produced by *Scaptotrigona bipunctata*; ATCC—American Type Culture Collection; MRSA—methicillin-resistant *Staphylococcus aureus*; (i)—isolated; (c)—in combination.

Against Gram-positive pathogens (*S. aureus* ATCC 25923, MRSA BMB9393, and *S. epidermidis* ATCC 12228), the combination produced consistent additive effects (FICI = 0.75). This interaction reduced the required concentrations of both agents two- to fourfold, from 1.25% to 0.31–0.62% *v*/*v* for SB honey and from 31.25–62.50 µM to 15.62 µM for bio-AgNP.

2.3. Time-Kill Antibacterial Kinetics

To evaluate the time course of the antibacterial effect, population survival curves were constructed over a 24-h exposure window. Against *E. coli* ATCC 25922 (Figure 1), the individual treatments reduced viable counts below the limit of detection (LOD; 2 $\log_{10}$ CFU/mL) within 4 h under bio-AgNP (125 µM) and within 7 h under SB honey (10% *v*/*v*). Their combination (31.25 µM bio-AgNP + 2.5% SB honey) reached the same endpoint at 4 h, despite using fourfold lower concentrations of both agents.

Against *S. aureus* ATCC 25923, viable counts fell below the LOD earlier under the combination than under either agent alone at its MBC (Figure 2). Isolated bio-AgNP (125 µM) and SB honey (2.5% *v*/*v*) required between 10 and 24 h for viable counts to drop below the LOD. Their combination (31.25 µM bio-AgNP + 1.25% SB honey) reduced viable

counts below the LOD by 7 h, with no recoverable colonies thereafter, using half the honey and one-quarter of the bio-AgNP concentration of the isolated treatments.

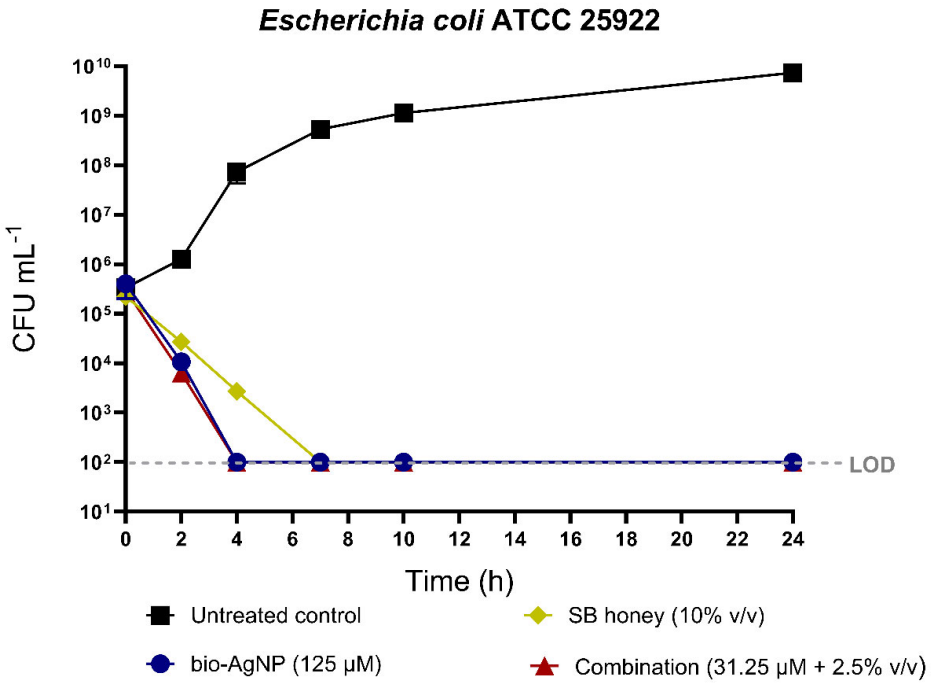


Figure 1. Time-kill kinetics of *Escherichia coli* ATCC 25922 exposed to isolated bio-AgNP (125 µM), isolated SB honey (10% *v*/*v*), and their combination (31.25 µM bio-AgNP + 2.5% SB honey) over 24 h. Data points represent mean ± SD of viable colony counts (CFU/mL, log scale) from three independent experiments. The dashed horizontal line indicates the limit of detection (LOD; 10^2 CFU/mL). Error bars, where not visible, are smaller than the symbol size.

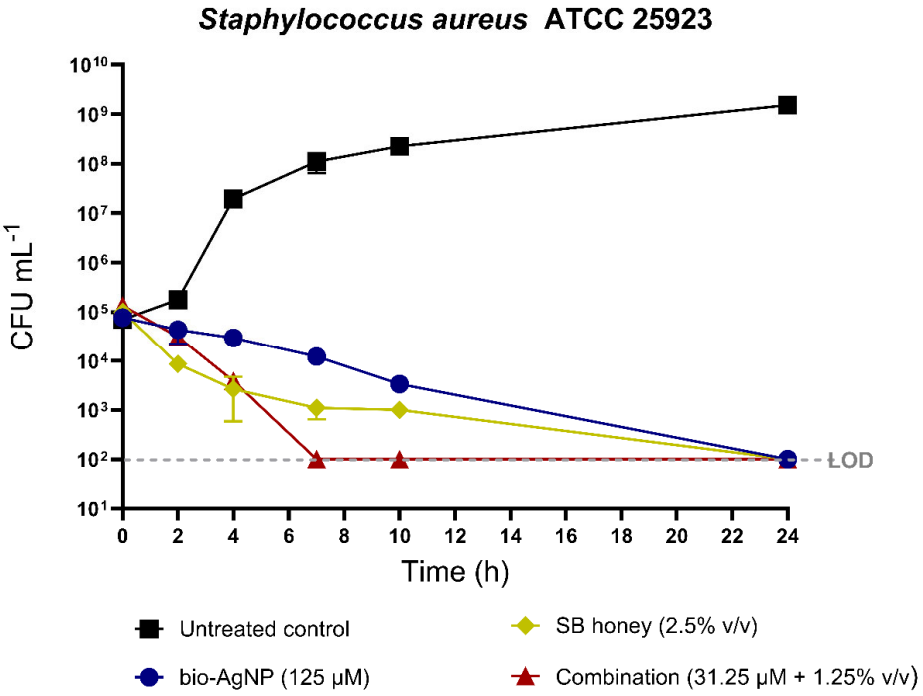


Figure 2. Time-kill kinetics of *Staphylococcus aureus* ATCC 25923 exposed to isolated bio-AgNP (125 µM), isolated SB honey (2.5% *v*/*v*), and their combination (31.25 µM bio-AgNP + 1.25% SB honey) over 24 h. Data points represent mean ± SD of viable colony counts (CFU/mL, log scale) from three independent experiments. The dashed horizontal line indicates the limit of detection (LOD; 10^2 CFU/mL). Error bars, where not visible, are smaller than the symbol size.

Because the starting inoculum of *S. aureus* was approximately 10^5 CFU/mL (Figure 2), reductions to below the LOD corresponded to approximately 3 $\log_{10}$, and the $\geq$ 3 $\log_{10}$ bactericidal criterion could not be formally assessed for this strain. The comparison between treatments is therefore based on the time required to reach the LOD from a common starting inoculum.

The most pronounced effect was observed against the clinical MDR *P. aeruginosa* 2491 isolate. In the 24-h design, all three treatments brought it below the LOD by the first sampling point (2 h; Figure 3a); the isolate was therefore re-tested over a shorter interval (Figure 3b), in which both individual agents required 60 min to drive viable counts below the LOD, whereas the combination (31.25 µM bio-AgNP + 2.5% SB honey) did so within 30 min. By 15 min, the combination had already reduced viable counts by 2.9 $\log_{10}$ (from 5.53 to 2.62 $\log_{10}$ CFU/mL), whereas the isolated bio-AgNP and SB honey had produced reductions of only 0.13 and 0.34 $\log_{10}$, respectively. All *P. aeruginosa* treatments satisfied the bactericidal criterion ($\geq$3 $\log_{10}$ reduction from the 0-h inoculum).

In the 24-h assays, untreated controls grew exponentially, exceeding 10^9 CFU/mL by 24 h (Figures 1, 2 and 3a). In the short-interval assay (Figure 3b), the untreated control remained viable but increased only slightly over 120 min (from approximately 2.5×10^5 to 7.7×10^5 CFU/mL), consistent with the lag phase that precedes exponential growth.

2.4. Surface Morphological Alterations via Scanning Electron Microscopy

For scanning electron microscopy, *S. aureus* ATCC 25923 was imaged at a higher cell density than that used in the susceptibility and time-kill assays and exposed for a fixed 3 h to fixed concentrations of each agent, conditions chosen to reveal morphological and field-scale changes rather than to reproduce inhibitory endpoints (Section 4.6). At low magnification (3000×; Figure 4), the distribution and coverage of cells across the field were examined, and at high magnification (50,000×; Figure 5), the surface morphology of individual cells.

At low magnification (3000×; Figure 4), untreated control cells (Figure 4a) formed a dense, near-confluent layer covering most of the substrate. Cells exposed to SB honey (Figure 4b) or bio-AgNP alone (Figure 4c) retained comparably high substrate coverage but were organized into discrete aggregates separated by wider channels of exposed substrate. The combination (Figure 4d) was the only condition showing a clear reduction in coverage, with sparsely distributed cells and extensive bare areas. This effect occurred even though each agent was present at a lower concentration than in its isolated treatment (half the honey and one-quarter the bio-AgNP).

At higher magnification (50,000×; Figure 5), control cells (Figure 5a) displayed a smooth, intact surface and turgid spherical morphology. At this scale, ultrastructural changes at the cell surface became apparent: cells treated with the individual agents (Figure 5b,c) largely retained their spherical shape but showed more numerous localized surface protrusions than the control, along with occasional amorphous cells that had lost the typical spherical outline (arrows). In the combination group (Figure 5d), these features were accompanied by a higher frequency of cells displaying incomplete division septa (arrowheads), consistent with the reduced coverage seen at low magnification.

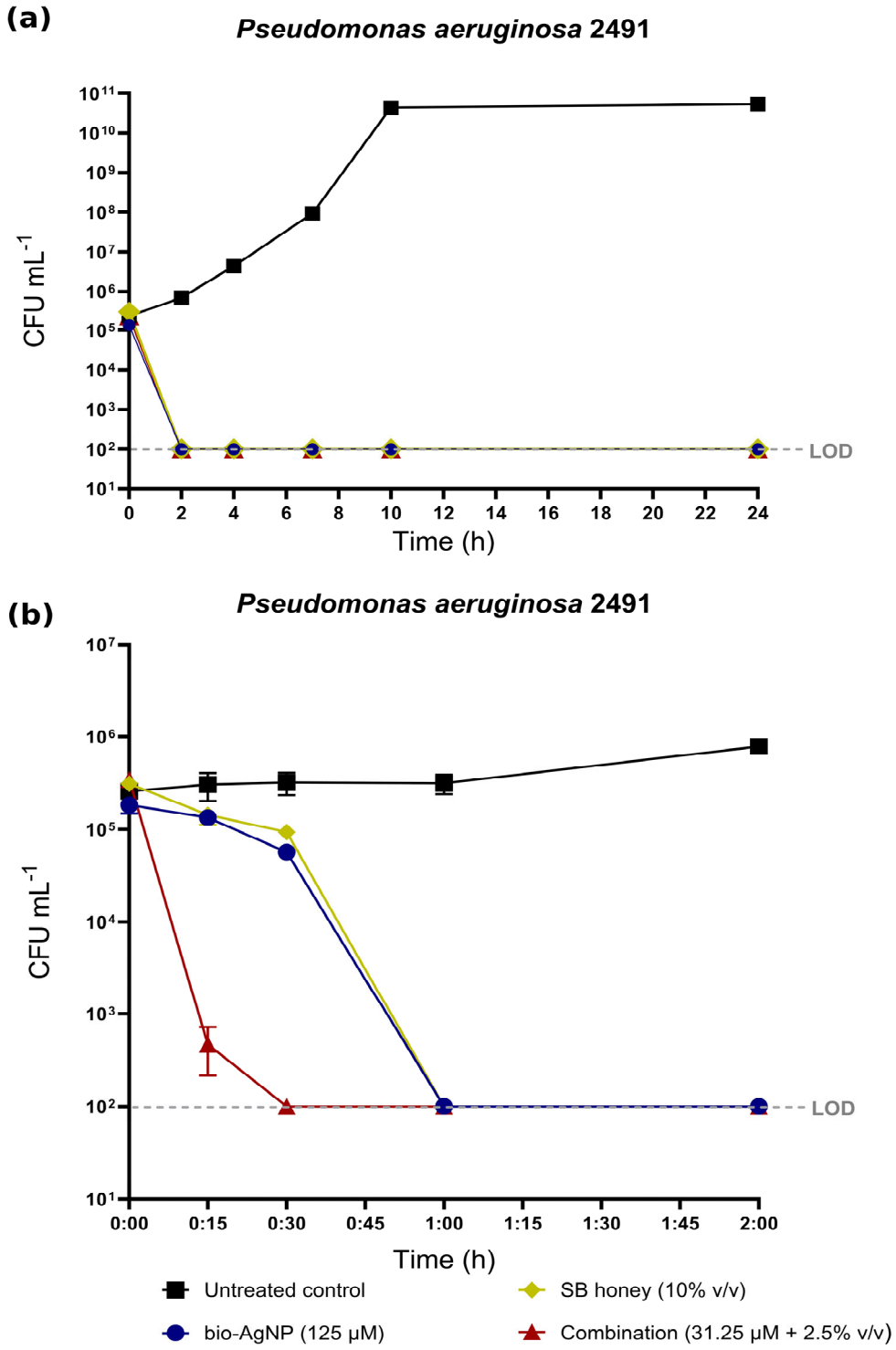


Figure 3. Time-kill kinetics of the clinical multidrug-resistant isolate *Pseudomonas aeruginosa* 2491 exposed to isolated bio-AgNP (125 µM), isolated SB honey (10% *v*/*v*), and their combination (31.25 µM bio-AgNP + 2.5% *v*/*v* SB honey). (**a**) 24-h experiment ($n = 1$), with sampling at 0, 2, 4, 7, 10 and 24 h. (**b**) Independent short-interval experiment, with sampling at 0, 15, 30, 60 and 120 min; data points represent the mean ± SD of viable counts (CFU/mL, log scale) from three independent experiments, each with an independently prepared inoculum. The dashed horizontal line indicates the limit of detection of the plating method (LOD; 10^2 CFU/mL). Error bars, where not visible, are smaller than the symbol size.

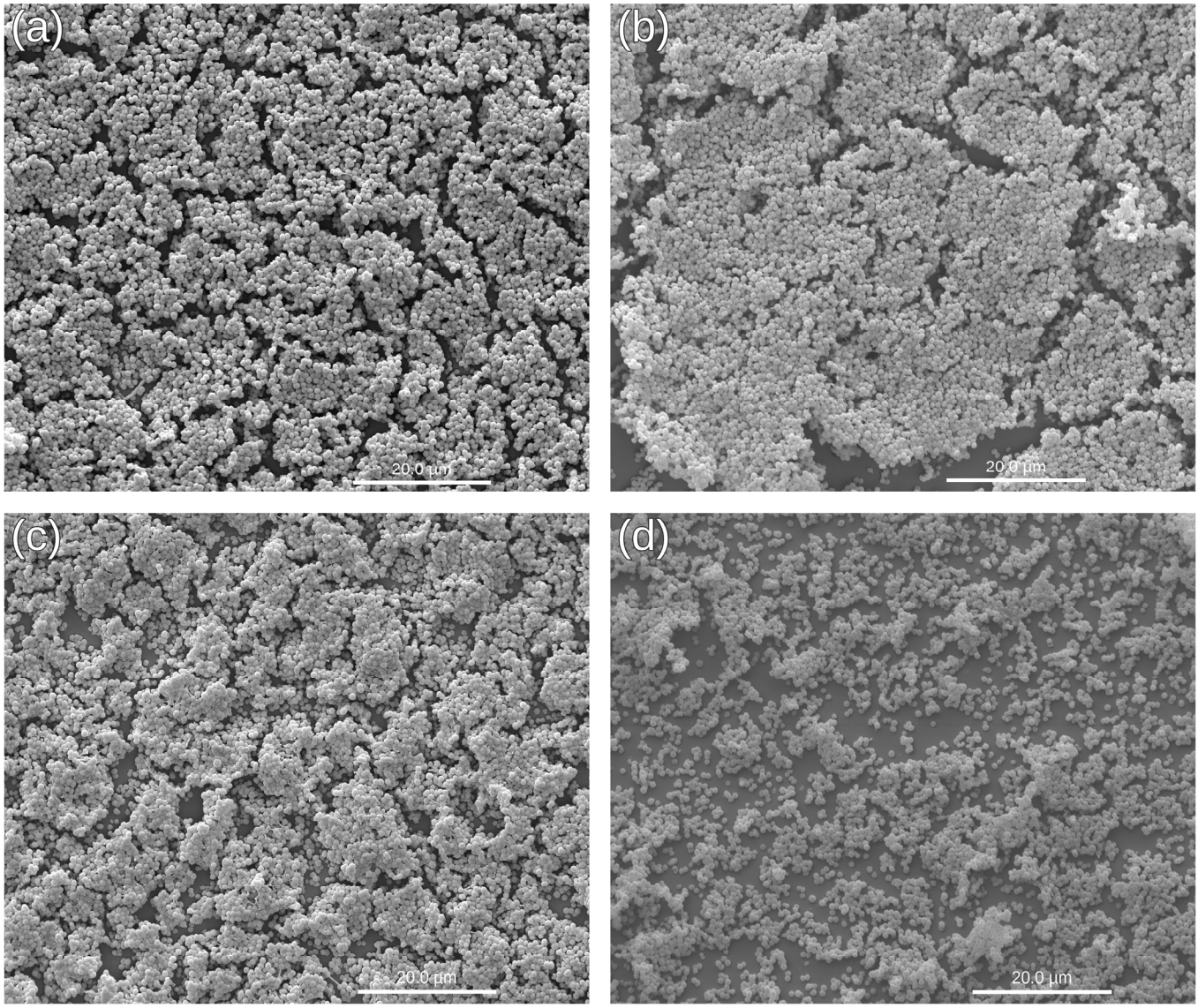


Figure 4. Low-magnification (3000×) scanning electron micrographs of *S. aureus* ATCC 25923 after 3 h of treatment. (**a**) Untreated control. (**b**) 1.25% (*v*/*v*) SB honey. (**c**) 125 µM bio-AgNP. (**d**) Combination of SB honey (0.62% *v*/*v*) and bio-AgNP (31.25 µM). Scale bars = 20 µm.

2.5. In Vitro Cytotoxicity and Selectivity

Cytotoxicity was determined for each agent alone in HaCaT keratinocytes. As presented in Table 3, the 50% cytotoxic concentration (CC_{50}) was 64.00 µM (95% confidence interval [CI]: 61.38–66.61) for bio-AgNPs and 7.79% *v*/*v* (95% CI: 6.94–8.63) for SB honey.

When evaluated against the MIC of each pathogen, the isolated agents generally yielded low selectivity indices (SI), with SI(i) values as low as 1.02 for bio-AgNPs and 1.56 for SB honey against several strains, indicating cytotoxic and inhibitory concentrations in a similar range. Because the combination lowered the required inhibitory concentration up to fourfold, the combination-based SI increased across all tested strains. For bio-AgNPs, the SI rose to 4.10 for most strains and reached 16.41 against *P. aeruginosa* ATCC 27853. For SB honey, the SI increased up to 24.92 against *S. epidermidis* ATCC 12228, indicating that, on a calculated basis, the concentrations required in combination fall below the cytotoxic threshold of each isolated agent.

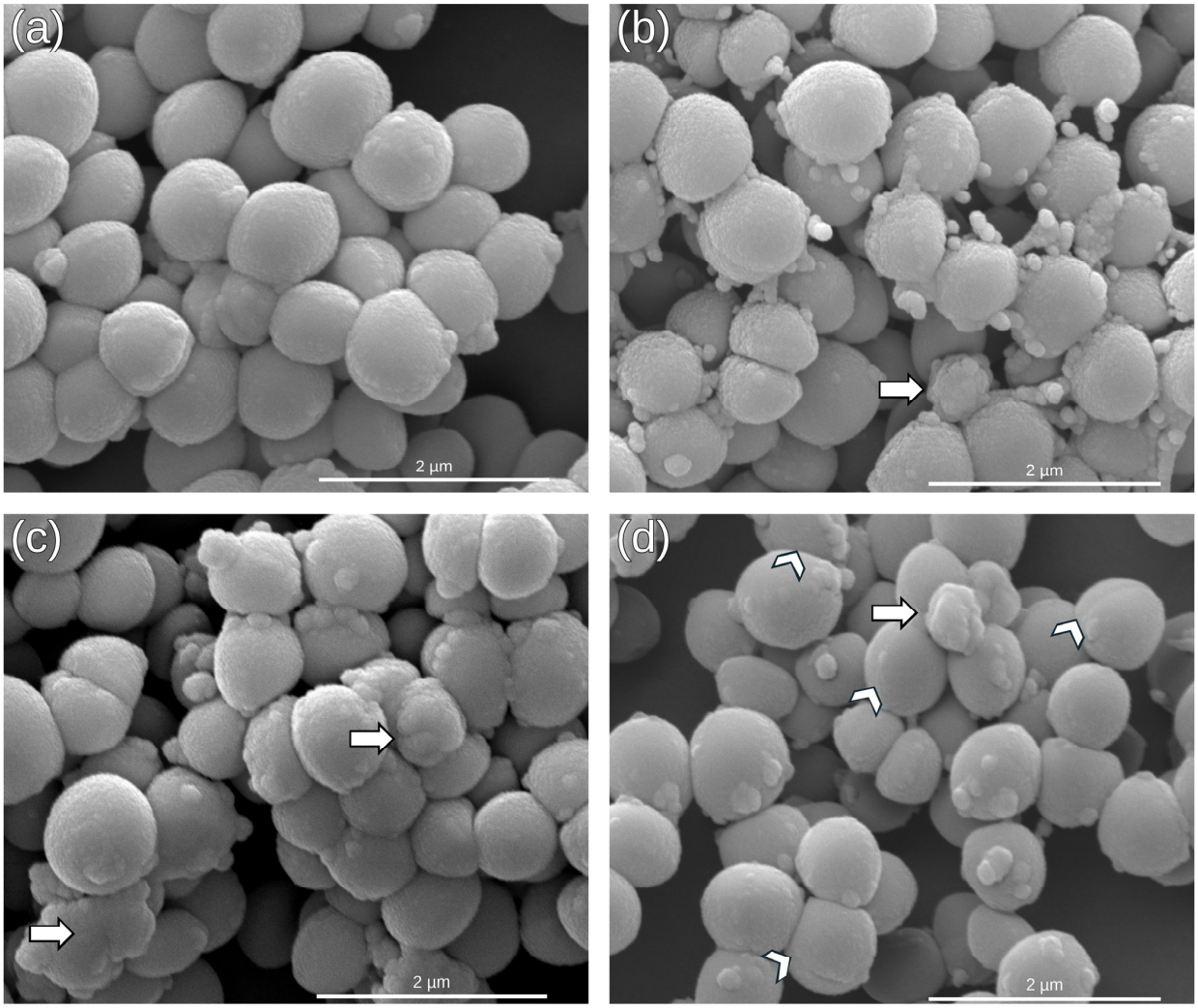


Figure 5. High-magnification (50,000×) scanning electron micrographs of *S. aureus* ATCC 25923 after 3 h of treatment. (**a**) Untreated control. (**b**) 1.25% (*v*/*v*) SB honey. (**c**) 125 µM bio-AgNP. (**d**) Combination of SB honey (0.62% *v*/*v*) and bio-AgNP (31.25 µM). White arrows indicate amorphous cells with loss of the typical spherical morphology; arrowheads indicate cells with incomplete division septa. Scale bars = 2 µm.

Table 3. Cytotoxic concentration for 50% of HaCaT keratinocytes (CC_{50}) and selectivity index (SI) of SB honey and bio-AgNP against reference and MDR strains, calculated from the MIC of each agent alone and in combination.

Bacterial Strain	Bio-AgNP CC_{50} = 64.00 µM (95% CI: 61.38–66.61)		SB Honey CC_{50} = 7.79% (95% CI: 6.94–8.63)	
	SI (i)	SI (c)	SI (i)	SI (c)
E. coli ATCC 25922	1.02	4.10	1.56	6.23
S. aureus ATCC 25923	1.02	4.10	6.23	12.56
MRSA BMB9393	1.02	4.10	6.23	12.56
S. epidermidis ATCC 12228	2.04	4.10	6.23	24.92
P. aeruginosa ATCC 27853	4.10	16.41	1.56	6.23
P. aeruginosa 2491	1.02	4.10	1.56	6.23

CC_{50}—cytotoxic concentration for 50% of the cells; SI—selectivity index (CC_{50}/MIC); ATCC—American Type Culture Collection; MRSA—methicillin-resistant *Staphylococcus aureus*; (i)—SI calculated relative to the MIC of the isolated compound; (c)—SI calculated relative to the MIC of the compound in combination. CC_{50} values are expressed with their 95% confidence interval (CI).

3. Discussion

Both conventional *Apis mellifera* and native stingless bee honeys (Meliponini) possess complex, multi-targeted antimicrobial compositions. However, the ultimate efficacy of a honey matrix is driven not only by its botanical source, but also by the specific entomological contributions of the bee species itself, since enzymatic secretions, endogenous peptides, and processing methods vary between species [27–29]. In this study, *Scaptotrigona bipunctata* (SB) honey demonstrated potent baseline activity, particularly against Gram-positive bacteria (MIC 1.25–2.5% *v*/*v*), inhibiting critical pathogens such as MRSA BMB9393 at concentrations where *A. mellifera* honey did not reach complete inhibition. Its advantage was not confined to Gram-positive targets: even against the Gram-negative MDR *E. coli* 5616, SB honey achieved complete inhibition (MIC 5.0% *v*/*v*), whereas *A. mellifera* honey did not inhibit it at the highest concentration tested (MIC >20% *v*/*v*). This differential susceptibility suggests that the specific biochemistry of native Meliponini honey may confer antibacterial advantages against these resistant isolates. The peroxide-dependent and non-peroxide factors that could account for this difference are considered in turn below.

A commonly proposed mechanism for honey's antibacterial activity relies on a balance between peroxide and non-peroxide components. Enzymatic generation of hydrogen peroxide (H_2O_2) is described as inducing oxidative stress, DNA degradation, and growth arrest [30,31]. As reported by Nishio et al. [32], the addition of catalase can drastically reduce honey's baseline activity against *S. aureus* and *E. coli*, in line with a contribution from hydrogen peroxide to the activity of those honeys.

Non-peroxide factors likely provide additional support and may help explain the differential efficacy observed between honey sources. Both SB and *A. mellifera* honeys exhibited similarly low pH values (SB 3.45 ± 0.09; *A. mellifera* 3.50 ± 0.10), which broadly contributes to disrupting the bacterial proton-motive force [33]; this alone, however, does not account for the superior potency of the SB honey.

Phenolic acids and flavonoids repeatedly reported in stingless bee honey, such as quercetin, *p*-coumaric, ferulic, and syringic acids, act largely at the cell envelope and on cytoplasmic targets such as DNA gyrase [34–38], the former consistent with the surface alterations later observed by electron microscopy. Although the present sample was not phytochemically characterized, these compounds are documented constituents of SB honey [9,39–41] and are proposed as plausible contributors to the antibacterial activity observed here.

Taken together, these proposed mechanisms are consistent with the profile observed in our own data: SB honey inhibited most Gram-positive strains at 1.25% (*v*/*v*), including *S. aureus*, MRSA BMB9393, and *S. epidermidis*, whereas most Gram-negative strains required 5.0%. Two strains departed from this grouping—*C. acnes* among the Gram-positives and *A. baumannii* among the Gram-negatives, both inhibited at 2.5%—indicating that the Gram stain predicts susceptibility only as a general tendency and that strain-level factors also contribute. Because these low-molecular-weight phenolics act at envelope and cytoplasmic targets, their reach depends on cell wall architecture: in Gram-positive bacteria the targets are shielded only by a porous, if thick, peptidoglycan layer, whereas in Gram-negative species the additional lipopolysaccharide-rich outer membrane imposes a selective permeability barrier that likely restricts their access [42,43]. This offers a plausible explanation for the generally lower MICs observed against Gram-positive targets, although the comparatively low MIC against *A. baumannii* ATCC 19606 (2.5% *v*/*v*) indicates that this barrier effect is not absolute and that susceptibility also varies at the strain level.

In contrast to the honey's profile, the bio-AgNPs were most active against Gram-negative strains: the lowest MIC was recorded against *P. aeruginosa* ATCC 27853 (15.62 μM), versus 62.5 μM for most Gram-positive strains, while *C. acnes* stood apart at 250 μM. This

high MIC is expected under the anaerobic conditions used to culture this species, since the antibacterial activity of AgNPs depends on the oxidative dissolution of silver to Ag^+, which is strongly attenuated in the absence of oxygen [44,45].

Nanoparticle activity at this scale is governed more by size and surface chemistry than by penetration of intact particles across the cell wall. The bio-AgNPs used here had a mean hydrodynamic diameter of 82.73 nm, far larger than the porin channels that gate solute passage across the Gram-negative outer membrane, which admit molecules only up to ~600 Da through pores on the order of 1 nm [46]; in *P. aeruginosa* and *A. baumannii* these channels are more restrictive still, excluding solutes above ~200 Da [46]. Entry of intact particles through this route is therefore implausible, and for particles well above 10 nm the predominant antibacterial contribution is understood to arise from the sustained release of Ag^+ through oxidative dissolution at the particle surface, rather than from the particle itself [47]. Released Ag^+ crosses the envelope and acts through electrostatic interaction with membrane proteins, generation of reactive oxygen species, binding to protein thiol groups, and interaction with nucleic acids [47]. The greater susceptibility of Gram-negative strains is in agreement with reports of stronger silver-mediated inhibition in Gram-negative than in Gram-positive bacteria [43], though the overlap in MIC ranges indicates a tendency rather than a rule.

Surface chemistry governs the first step of this process. The bio-AgNPs carried a zeta potential of −23.27 mV, a moderate negative charge expected to produce electrostatic repulsion against the equally electronegative bacterial surface. The fact that activity is retained despite this repulsion points to a compensatory role for the capping layer derived from the *Trichilia catigua* bark extract. As reported by Ferreyra Maillard et al. [48], hydrophobic and aromatic moieties in biogenic capping layers interact favorably with membrane lipid head groups, promoting attachment and membrane destabilization.

When SB honey and bio-AgNPs are combined, more than one mechanism could contribute to the interaction observed in the checkerboard assay. One is a localized Fenton-like reaction, in which hydrogen peroxide from the honey matrix reacts with silver ions shed by the bio-AgNPs to form hydroxyl radicals, which would amplify oxidative stress beyond either agent alone [49]. This pathway is chemically plausible but was not tested here.

A further mechanism that may contribute is a reciprocal permeabilization of the bacterial envelope, consistent with the concentration reductions observed here. *p*-Coumaric acid, one of the main phenolic compounds reported in SB honey [9,39], compromises bacterial membrane integrity and barrier function, causing leakage of cytoplasmic contents [35], an effect shared to varying degrees by other honey-associated phenolic acids such as ferulic, protocatechuic, and syringic acid [50]. At the concentrations reached in monotherapy, this permeabilization is likely only partial, weakening without abolishing the outer-membrane barrier, which would predict the honey's higher MICs. In combination, the two agents may relieve each other's principal barrier: the partial phenolic-mediated permeabilization lowers the threshold for Ag^+ entry, while the membrane permeabilization driven by the nanoparticles, which is known to enhance the intracellular access of co-administered antibacterial agents [51], in turn facilitates the access of honey-derived phenolics to their targets. This reciprocal relief offers a rationale for the reduced concentrations of both agents required in combination and parallels the synergistic FICI values obtained against the Gram-negative strains (Table 2), in which the outer membrane is the principal barrier.

The classification of the Gram-positive results depends on the interpretive scheme adopted: under the more conservative criteria proposed by Odds [52], in which $0.5 < \text{FICI} \leq 4$ indicates no interaction, these combinations would be classified as indifferent, whereas the synergistic classification of the Gram-negative results ($\text{FICI} \leq 0.5$) is unaffected.

These mechanisms may also help explain why earlier honey–silver combinations have yielded variable results. Taherpour et al. [26] recorded no synergy, only additivity against *E. coli* and indifference against the remaining strains, whereas Senanayake et al. [25] reported synergy against Gram-negative species (FICI 0.44–0.48) as observed here. In both studies, the nanoparticles were chemically synthesized (citrate or borohydride reduced) rather than biogenic, and the honey was of honeybee or undeclared origin. If the interaction depends jointly on the capping-mediated membrane association of the nanoparticles and on the peroxide activity and phenolic profile of the honey, its occurrence and magnitude are likely to vary with the specific partners combined.

The combination also acted rapidly. Containing each agent at half its isolated MIC (Table 1), it reduced viable counts of MDR *P. aeruginosa* 2491 below the LOD within 30 min, a $\geq$3 $\log_{10}$ reduction from the starting inoculum (Figure 3b), and those of *E. coli* ATCC 25922 within 4 h (Figure 1). Against *S. aureus*, counts fell below the LOD within 7 h (Figure 2). This speed of action is relevant to burn wound management, where the immediate loss of the skin barrier and accompanying immune suppression open a narrow window for opportunistic colonization: virulent *S. aureus* releases collagenases and hyaluronidases that promote local tissue invasion [53], and MRSA has become a predominant pathogen in burn units [54].

Because attachment and extracellular polymeric substance production begin within hours of surface contact [55], a treatment that shortens the interval in which viable cells persist may correspondingly narrow the window available for surface colonization. This margin would be species-dependent (Figures 2 and 3b). Beyond speed of action, combining biogenic AgNPs with agents acting through distinct pathways has been reported to restrict the emergence of resistance that the nanoparticle alone selects for over repeated exposure [56].

Scanning electron microscopy of *S. aureus* provided a qualitative morphological counterpart to these kinetic findings: despite lower concentrations of both agents than in the isolated treatments, the combination was the only condition showing a clear reduction in cell coverage. Localized surface protrusions were visible across all treated groups: isolated SB honey, isolated bio-AgNP, and their combination alike. This is consistent with the classic cellular stress response in which structural integrity is compromised and cytoplasmic material begins to leak [57]. What set the combined treatment apart was not the presence of these protrusions, which occurred under every condition, but the reduced cell density noted above, accompanied by a higher frequency of cells displaying incomplete division septa. Notably, honey has been reported to interfere with bacterial cell separation: Henriques et al. [58] observed that exposed cells can form the division septum but fail to complete separation, possibly through inhibition of enzymes required for cell cleavage. Whether a similar process underlies the incomplete septa observed here, and whether they reflect a genuine effect on cell division, remains to be established.

Beyond mechanism and kinetics, a central translational question for any combination therapy is whether increased efficacy comes at the cost of increased host toxicity. This concern is well illustrated by silver sulfadiazine, still one of the most widely used topical antimicrobials in burn care, whose free silver ions can damage human dermal fibroblasts and epidermal keratinocytes and potentially delay re-epithelialization [59]. It thus offers a familiar point of reference for the trade-off examined here. Our cytotoxicity assays showed that, used alone, both bio-AgNPs and SB honey required concentrations close to their respective CC_{50} values to achieve inhibitory activity, yielding selectivity indices near 1 for several strains, an unfavorable margin for topical use.

Because the concentration required for inhibitory activity dropped substantially in combination, the selectivity indices expanded accordingly. For the bio-AgNPs, the index

rose from approximately 1 in monotherapy to 4.10 across most strains, including the multidrug-resistant MRSA BMB9393 and *P. aeruginosa* 2491, and reached 16.41 against the susceptible reference strain *P. aeruginosa* ATCC 27853. For SB honey, it rose from a range of 1.56–6.23 to 6.23–24.92. The improvement was observed in both MDR isolates tested (MRSA BMB9393 and *P. aeruginosa* 2491) as well as in the reference strains, rather than confined to any single strain. Within the concentration ranges tested in this in vitro keratinocyte model, the calculated margin between antibacterial and cytotoxic concentrations was wider for the combination than for either agent alone. Whether this translates into a genuine safety advantage over silver sulfadiazine or other current topical antimicrobials would require direct comparative testing under matched conditions, including in vivo wound-healing models.

Three boundaries frame the interpretation of these results. First, the mechanisms proposed above were inferred from the established chemistry of both agents rather than tested directly; targeted assays separating the phenolic, peroxide, and capping contributions, ideally paired with phytochemical characterization of the honey across batches, are needed to confirm them. Second, the time-kill assays were designed to describe killing kinetics at equivalent multiples of the MIC and did not include each agent alone at its concentration in the combination; they therefore do not quantify the interaction between the agents, which was assessed here by the checkerboard assay. Third, cytotoxicity was determined for each agent separately, so the selectivity indices for the combination are calculated under an assumption of non-interactive cytotoxicity; measuring the combination directly would refine these estimates. Beyond these, the study is entirely in vitro, and validation in ex vivo or in vivo wound models remains the necessary step before the combination's therapeutic margin can be claimed as a clinical advantage.

4. Materials and Methods

4.1. Bacterial Strains and Culture Conditions

The individual and combined antibacterial activities were evaluated using reference strains and MDR isolates relevant to skin and wound infections. The reference panel comprised four Gram-positive strains, *Staphylococcus aureus* ATCC 25923, *Staphylococcus epidermidis* ATCC 12228, *Streptococcus pyogenes* ATCC 19615 and *Cutibacterium acnes* ATCC 6919, and four Gram-negative strains, *Escherichia coli* ATCC 25922, *Pseudomonas aeruginosa* ATCC 27853, *Acinetobacter baumannii* ATCC 19606 and *Klebsiella pneumoniae* ATCC 10031. All reference strains were held by the Laboratory of Basic and Applied Bacteriology (LBBA), Department of Microbiology, State University of Londrina (UEL), Londrina, PR, Brazil. Unless otherwise stated, strains were cultured and assayed aerobically at 37 °C; *C. acnes* ATCC 6919 was cultured and assayed under anaerobic conditions using a GasPak system at 37 °C.

Three clinical MDR isolates were also included: methicillin-resistant *S. aureus* (MRSA) BMB9393, belonging to the Brazilian Epidemic Clone lineage; *P. aeruginosa* 2491, a hospital-acquired urinary tract isolate obtained from the University Hospital (Hospital das Clínicas, Londrina, PR, Brazil); and *E. coli* 5616, a urinary-tract isolate provided by the Adolfo Lutz Institute (São Paulo, SP, Brazil). All three clinical isolates met the criteria for multidrug resistance [60]: the two Gram-negative isolates were non-susceptible to agents in at least three antimicrobial categories, and MRSA is considered MDR by definition, as oxacillin resistance predicts non-susceptibility to all β-lactam categories. Their full resistance profiles are given in Table 4.

Table 4. Antimicrobial resistance profiles and provenance of the clinical multidrug-resistant isolates used in this study.

Isolate	Origin/ Donor Source	Resistance Profile (Agent; Antimicrobial Category)	Classification
MRSA BMB9393	Brazilian Epidemic Clone lineage; LBBA collection, UEL	Methicillin/oxacillin (β-lactams), defining the MRSA phenotype.	MRSA
P. aeruginosa 2491	Urinary tract infection; Hospital das Clínicas, Londrina, PR (Prof. F. E. Carrara Marroni)	Amikacin, gentamicin (aminoglycosides); ciprofloxacin, levofloxacin (fluoroquinolones); cefepime, ceftazidime (antipseudomonal cephalosporins); imipenem, meropenem (carbapenems); piperacillin–tazobactam (β-lactam/β-lactamase-inhibitor)	MDR (≥5 categories)
E. coli 5616	Urinary tract infection; Adolfo Lutz Institute, São Paulo, SP	Ampicillin (penicillins); amoxicillin–clavulanate, ampicillin–sulbactam, piperacillin–tazobactam (β-lactam/β-lactamase-inhibitor combinations); cefazolin, cefuroxime, cefpodoxime, ceftriaxone (cephalosporins, 1st–3rd gen.); aztreonam (monobactams); imipenem, meropenem (carbapenems); sulfonamides (folate-pathway inhibitors); fosfomycin (phosphonic acids)	MDR (≥7 categories)

MRSA—methicillin-resistant *Staphylococcus aureus*; MDR—multidrug-resistant (non-susceptible to ≥1 agent in ≥3 antimicrobial categories, per Magiorakos et al. [60]).

All strains were preserved in Brain Heart Infusion broth supplemented with 20% (*v*/*v*) glycerol and stored at −20 °C. For the *P. aeruginosa* isolates, working stocks were additionally maintained as stab cultures at room temperature, with cryopreserved backups held at −80 °C.

4.2. Acquisition of Honeys and Biogenic Silver Nanoparticles

Honeys from three native stingless bee species (*Tetragonisca angustula*, *Scaptotrigona bipunctata*, and *Tetragona clavipes*) came from a private meliponary in Londrina, PR, Brazil (23°18′50″ S, 51°17′19″ W), and *Apis mellifera* honey from an apiary in Sertaneja, PR, Brazil (23°02′17″ S, 50°47′39″ W); all were harvested in February 2020. Samples were diluted to 50% (*v*/*v*) in sterile distilled water, sterilized by filtration through a 0.22 µm membrane and stored until use at 4 °C (stingless bee honeys) or at room temperature (*A. mellifera* honey). The pH of each undiluted honey was measured in triplicate at room temperature with a calibrated pH meter (Starter ST2200-F; OHAUS Corporation, Parsippany, NJ, USA).

Biogenic silver nanoparticles (bio-AgNPs) were provided by GRAL Bioativos Ltda. (Londrina, Brazil), where they were synthesized biologically from an aqueous bark extract of *Trichilia catigua*, following the patented protocol (BR 10 2021 016375 5) [61]. Physicochemical characterization was performed for the manufacturer by the Technological Research Institute (IPT, São Paulo, Brazil) using dynamic light scattering and electrophoretic light scattering (Zetasizer Nano, Malvern Instruments, Malvern, UK). The bio-AgNPs had a mean hydrodynamic diameter of 82.73 nm, a polydispersity index of 0.17, and a zeta potential of −23.27 mV.

The same batch of bio-AgNPs used in this study was further characterized in previous studies: transmission electron microscopy, performed at the State University of Maringá

on a JEM-1400 microscope (JEOL Ltd., Tokyo, Japan), showed particles of approximately 80–100 nm surrounded by an organic coating consistent with the plant-derived capping layer [62,63], and X-ray diffraction showed peaks characteristic of crystalline silver [62]. The ultraviolet–visible (UV-Vis) spectrum of the same batch, recorded after storage at 4 °C in the dark, showed a surface plasmon resonance band at 457 nm (Figure S1).

The pH measurements and all antibacterial, scanning electron microscopy and cytotoxicity assays were performed between February 2021 and January 2022.

4.3. Determination of Minimum Inhibitory (MIC) and Bactericidal (MBC) Concentrations

MIC values were determined via the broth microdilution method in 96-well plates following Clinical and Laboratory Standards Institute (CLSI, [64]) guidelines. Honeys were assayed as two-fold serial dilutions ranging from 0.1562% to 20% (v/v), and bio-AgNPs from 3.9 to 500 µM. Bacterial suspensions were prepared in saline solutions, standardized to 0.5 McFarland standard (equivalent to 1.5×10^8 colony-forming units (CFU)/mL), diluted 1:100 in Mueller–Hinton (MH) broth (Difco, BD, Sparks, MD, USA), and inoculated into wells to achieve a final density of 5.0×10^5 CFU/mL. Microplates were incubated at 37 °C for 24 h (48 h under anaerobic conditions for *C. acnes*, as described in Section 4.1). Positive (inoculated broth without treatment) and negative (sterile broth with treatment) controls were included. Growth was assessed visually at the end of incubation and scored against the corresponding treatment-only sterility control at the same concentration, which served as the turbidity and color blank for each honey and bio-AgNP dilution. The MIC was defined as the lowest concentration showing no visible growth relative to this blank.

The MBC was determined by subculturing 10 µL from the MIC well and from all wells corresponding to higher concentrations onto MH agar (Difco, BD, Sparks, MD, USA). Plates were incubated at 37 °C for 24 h (48 h under anaerobic conditions for *C. acnes*), and the MBC was defined as the lowest concentration that eliminated $\geq$ 99.9% of the initial bacterial inoculum (National Committee for Clinical Laboratory Standards, NCCLS [65]).

4.4. Checkerboard Synergy Assays

The antibacterial interaction between SB honey and bio-AgNPs was assessed by broth microdilution using a double concentration gradient of both agents, following a modified checkerboard method [66,67]. In 96-well plates, SB honey was serially diluted along one axis and bio-AgNPs along the other, generating all pairwise combinations of the two agents. Bacterial suspensions were standardized in sterile saline (0.85% NaCl) to the 0.5 McFarland turbidity standard (1.5×10^8 CFU/mL) and diluted 1:100 in Mueller–Hinton broth before inoculation, reaching a final density of 5.0×10^5 CFU/mL per well. Sterility and growth controls were included, and plates were incubated at 37 °C for 24 h.

The fractional inhibitory concentration (FIC) of each agent was calculated by dividing its MIC in combination by its MIC alone, and the fractional inhibitory concentration index (FICI) was obtained as the sum of the two individual FICs (Equation (1)) [67,68]. Interactions were classified as synergistic (FICI $\leq$ 0.5), additive (0.5 < FICI $\leq$ 1), indifferent (1 < FICI < 2), or antagonistic (FICI $\geq$ 2) [67,68]. In each plate, the MIC of each agent alone was determined in duplicate alongside the checkerboard, and the FICI of each replicate was calculated relative to these values.

$$\mathrm{FICI} = \mathrm{FIC_A} + \mathrm{FIC_B} = \frac{\mathrm{MIC_{A\ in\ combination}}}{\mathrm{MIC_{A\ alone}}} + \frac{\mathrm{MIC_{B\ in\ combination}}}{\mathrm{MIC_{B\ alone}}} \quad (1)$$

4.5. Time-Kill Population Kinetics

Time-dependent bactericidal effects were assessed by viable cell counting, adapted from NCCLS document M26-A [65]. Three representative strains were selected: a Gram-

positive reference (*S. aureus* ATCC 25923), a Gram-negative reference (*E. coli* ATCC 25922), and a clinically relevant multidrug-resistant isolate (MDR *P. aeruginosa* 2491). Bacterial suspensions were prepared in sterile saline (0.85% NaCl), standardized to the 0.5 McFarland turbidity standard (1.5×10^8 CFU/mL), and diluted 1:100 in Mueller–Hinton (MH) broth to a starting inoculum of approximately 5×10^5 CFU/mL. Cultures were exposed to each agent alone at its MBC, which corresponded to twice its MIC (Table 1), and to the combination at twice the combination MIC (Table 2), alongside an untreated growth control.

Aliquots were withdrawn at 0, 2, 4, 7, 10 and 24 h, serially diluted in saline, and spot-plated (10 µL, in triplicate) on MH agar; colonies were counted after 18 h at 37 °C and the starting density was confirmed by the 0-h viable counts. Because MDR *P. aeruginosa* 2491 was cleared before the first post-treatment time point of this design, a short-interval experiment was subsequently carried out for this isolate alone, using an independently prepared inoculum and sampling at 0, 15, 30, 60 and 120 min. Both designs are reported for MDR *P. aeruginosa* 2491 (Figure 3a,b); *E. coli* ATCC 25922 and *S. aureus* ATCC 25923 were assessed under the 24-h design only (Figures 1 and 2).

Results are expressed as the mean ± SD of the resulting viable counts. The LOD of the plating method was 100 CFU/mL (2 $\log_{10}$ CFU/mL). Bactericidal activity was defined as a $\geq$3 $\log_{10}$ reduction in viable counts relative to the 0-h inoculum (NCCLS [65]). Time points from which no colonies were recovered are reported as values below the LOD rather than as complete elimination of the bacterial population.

4.6. Scanning Electron Microscopy (SEM)

Morphological and topographical changes were evaluated as previously described [69], with modifications. Because SEM requires sufficient surface cell density to obtain representative fields, *S. aureus* ATCC 25923 was prepared at an initial density of 10^8 CFU/mL in MH broth—higher than the 5×10^5 CFU/mL used in the susceptibility and time-kill assays, though lower than the 10^9 CFU/mL of the original protocol. As MIC and MBC were determined at the standard 5×10^5 CFU/mL inoculum, cells at this higher density were exposed to fixed concentrations selected to ensure a detectable morphological effect rather than to the MIC or MBC values: isolated SB honey at 1.25% (*v*/*v*), isolated bio-AgNP at 125 µM, and their combination at 0.62% (*v*/*v*) honey + 31.25 µM bio-AgNP, alongside an untreated control. All conditions shared the same starting inoculum and were incubated at 37 °C for a fixed 3 h period (versus the treatment-dependent times of 30 min to 6 h in the original protocol). After incubation, 10 µL of each suspension was deposited onto glass coverslips (instead of glass slides) pre-coated with 1% poly-L-lysine (Sigma-Aldrich, St. Louis, MO, USA).

Samples were fixed in 0.1 M sodium cacodylate buffer (pH 7.2) containing 2.5% (*v*/*v*) glutaraldehyde and 2% (*v*/*v*) paraformaldehyde for 20 h at 4 °C. Fixed cells underwent graded dehydration in an ethanol series (70%, 80%, 90%, and 100% *v*/*v*), critical-point drying with CO_2 (CPD 030; BAL-TEC AG, Balzers, Liechtenstein), and gold sputter-coating (SCD 050; BAL-TEC AG, Balzers, Liechtenstein) before topographical observation using an FEI Quanta 200 scanning electron microscope (FEI Company, Hillsboro, OR, USA).

4.7. In Vitro Cytotoxicity and Selectivity Index

The cytotoxic profiles of the isolated agents were screened against the immortalized human keratinocyte cell line (HaCaT; kindly provided by the Laboratory of Virology, Universidade Estadual de Londrina) via colorimetric 3-(4,5-dimethylthiazol-2-yl)-2,5-diphenyltetrazolium bromide (MTT; Sigma-Aldrich, St. Louis, MO, USA) assays based on ISO 10993-5 [70] guidelines. Cells were seeded in 96-well plates at an initial density of 1×10^4 cells per well in Dulbecco's Modified Eagle Medium (DMEM; Sigma-Aldrich,

St. Louis, MO, USA) and incubated at 37 °C under 5% CO_2 to establish a confluent monolayer. The medium was subsequently replaced with DMEM containing treatments of honey (0.1953% to 25% *v*/*v*) or bio-AgNPs (0.78 to 100 µM).

After 24 h of exposure, the treatment medium was completely removed from all wells to prevent direct chemical interaction between honey constituents and the tetrazolium salt, and 50 µL of MTT solution (5 mg/mL in phosphate-buffered saline) was added to each well for a 4-h incubation. Formazan crystals were solubilized with 100 µL of isopropanol per well, and plates were agitated for 30 min before reading. Absorbance was recorded at 570 nm with a 690 nm reference wavelength to correct for background and non-specific turbidity, in a Synergy HT microplate reader (BioTek Instruments, Winooski, VT, USA) running Gen5 software (version 2.01.14). Cell viability was expressed as a percentage of the untreated control, and the 50% cytotoxic concentration (CC_{50}) was calculated using linear regression analyses.

The selectivity index (SI) was calculated as the ratio of the CC_{50} of each isolated agent to the corresponding bacterial MIC, determined both for the agent alone and for the agent in combination. A higher SI reflects a wider safety window, with SI > 1 indicating that antibacterial activity occurs below the cytotoxic threshold [71].

4.8. Statistical Analysis

Unless otherwise stated, antibacterial assays were performed in three independent biological replicates. Minimum Inhibitory Concentration (MIC), Minimum Bactericidal Concentration (MBC) and Fractional Inhibitory Concentration Index (FICI) values are reported as the mode, in accordance with CLSI (2018) [64] recommendations; this reflects the discrete, two-fold dilution nature of these assays rather than a continuous variable amenable to parametric testing. Time-kill kinetics are expressed as the mean ± standard deviation (SD) of viable colony counts (CFU/mL), with error bars shown in Figures 1–3. Cytotoxicity (MTT) assays were performed in triplicate; CC_{50} values were obtained by linear regression (Microsoft Excel; version 2019; Microsoft Corporation, Redmond, WA, USA), and the mean CC_{50} and its 95% confidence interval were calculated across the three replicates from Student's t-distribution, using Python (version 3.13.16; Python Software Foundation, Wilmington, DE, USA) with SciPy (version 1.18.1).

5. Conclusions

Combining biogenic silver nanoparticles with *Scaptotrigona bipunctata* honey produced synergistic antibacterial effects against the Gram-negative strains and additive effects against the Gram-positive strains among the six strains tested in combination, including the MDR isolates MRSA BMB9393 and *P. aeruginosa* 2491. In every case, the combination lowered the concentrations of both agents required for inhibition. In the time-kill assays, at a fraction of the concentrations of the isolated treatments, it brought viable counts below the LOD faster than either agent alone against MDR *P. aeruginosa* 2491 and *S. aureus*, and as fast as the fastest single agent against *E. coli*. Scanning electron microscopy of *S. aureus* revealed surface disruption and a higher frequency of cells with incomplete division septa. The reduced concentrations required in combination also fell below the cytotoxic threshold of each isolated agent, increasing the calculated selectivity index.

Together, these results establish in vitro that two biologically derived agents can be combined to retain antibacterial activity against the reference and MDR strains tested, all associated with burn wound infections, at substantially reduced doses of each. Validation in ex vivo or in vivo wound models, together with compositional characterization of the honey matrix, represents the next step toward a clinically applicable formulation.

6. Patents

A Brazilian patent application covering the nanoparticle–honey composition reported here has been filed with the Instituto Nacional da Propriedade Industrial (INPI): "Composição de nanopartículas de prata com mel de abelhas sem ferrão" (Composition of silver nanoparticles with stingless bee honey), application No. BR 10 2026 009921 0, filed on 24 April 2026 by Universidade Estadual de Londrina (UEL).

Supplementary Materials: The following supporting information can be downloaded at: https://www.mdpi.com/article/10.3390/antibiotics15111054/s1, Figure S1: UV-Vis spectrum of the bio-AgNP batch used in the antibacterial assays; Table S1: FICI of each independent checkerboard replicate, calculated relative to the MIC of each agent alone determined on the same plate.

Author Contributions: Conceptualization, M.A.P., G.N. and R.K.T.K.; methodology, M.A.P., S.S. and M.C.G.; investigation, M.A.P. and L.P.M.; formal analysis, M.A.P.; visualization, M.A.P., L.P. and A.N.D.; writing—original draft preparation, M.A.P., L.P. and A.N.D.; writing—review and editing, S.S., G.N. and R.K.T.K.; supervision, M.C.G., G.N. and R.K.T.K.; project administration, G.N.; funding acquisition, G.N. and R.K.T.K. All authors have read and agreed to the published version of the manuscript.

Funding: This study was financed in part by the Coordenação de Aperfeiçoamento de Pessoal de Nível Superior–Brasil (CAPES)–Finance Code 001. The APC was funded by the Financiadora de Estudos e Projetos (FINEP), Brazil, through the Materiais Avançados program (Project BioAgNPLED; grant No. 01.22.0200.0, Ref. 0161/2021). The Conselho Nacional de Desenvolvimento Científico e Tecnológico (CNPq), Brazil, also provided scholarships to some of the authors.

Institutional Review Board Statement: Not applicable.

Informed Consent Statement: Not applicable.

Data Availability Statement: All data supporting the findings are included in the article (Tables 1–4 and Figures 1–5) and in the Supplementary Materials (Figure S1 and Table S1); additional raw data are available from the corresponding author upon reasonable request.

Acknowledgments: The authors thank the Laboratory of Basic and Applied Bacteriology and the Laboratory of Electron Microscopy and Microanalysis (LMEM) of the State University of Londrina.

Conflicts of Interest: G.N., R.K.T.K. and M.C.G. hold equity in GRAL Bioativos Ltda., which holds the patent on the bio-AgNPs (BR 10 2021 016375 5); the company's role was limited to supplying the nanoparticles. M.A.P., S.S., M.C.G., A.N.D., R.K.T.K. and G.N. are inventors on patent application BR 10 2026 009921 0 (Universidade Estadual de Londrina), which covers the composition reported here. The other authors declare no conflicts of interest.

Abbreviations

The following abbreviations are used in this manuscript:

AgNP	Silver nanoparticle
ATCC	American Type Culture Collection
bio-AgNP	Biogenic silver nanoparticle
CC_{50}	50% cytotoxic concentration
CFU	Colony-forming unit
CI	Confidence interval
CLSI	Clinical and Laboratory Standards Institute
DMEM	Dulbecco's Modified Eagle Medium
FIC	Fractional inhibitory concentration
FICI	Fractional inhibitory concentration index
HaCaT	Human immortalized keratinocyte cell line
LOD	Limit of detection

MBC	Minimum bactericidal concentration
MDR	Multidrug-resistant
MH	Mueller–Hinton (broth/agar)
MIC	Minimum inhibitory concentration
MRSA	Methicillin-resistant *Staphylococcus aureus*
MTT	3-(4,5-dimethylthiazol-2-yl)-2,5-diphenyltetrazolium bromide
NCCLS	National Committee for Clinical Laboratory Standards (now CLSI)
SB	*Scaptotrigona bipunctata* (honey)
SD	Standard deviation
SEM	Scanning electron microscopy
SI	Selectivity index
UV-Vis	Ultraviolet–visible (spectroscopy)

References

1. Naghavi, M.; Vollset, S.E.; Ikuta, K.S.; Swetschinski, L.R.; Gray, A.P.; Wool, E.E.; Robles Aguilar, G.; Mestrovic, T.; Smith, G.; Han, C.; et al. Global Burden of Bacterial Antimicrobial Resistance 1990–2021: A Systematic Analysis with Forecasts to 2050. *Lancet* **2024**, *404*, 1199–1226. [CrossRef] [PubMed]
2. Lachiewicz, A.M.; Hauck, C.G.; Weber, D.J.; Cairns, B.A.; Van Duin, D. Bacterial Infections After Burn Injuries: Impact of Multidrug Resistance. *Clin. Infect. Dis.* **2017**, *65*, 2130–2136. [CrossRef] [PubMed]
3. Elsheikh, R.; Makram, A.M. Multidrug-Resistant Organisms: The Silent Plight of Burn Patients. *J. Burn Care Res.* **2024**, *45*, 877–886. [CrossRef] [PubMed]
4. Hemmati, J.; Azizi, M.; Asghari, B.; Arabestani, M.R. Multidrug-Resistant Pathogens in Burn Wound, Prevention, Diagnosis, and Therapeutic Approaches (Conventional Antimicrobials and Nanoparticles). *Can. J. Infect. Dis. Med. Microbiol.* **2023**, *2023*, 8854311. [CrossRef] [PubMed]
5. Dadashizadeh, G.; Elloso, M.; Jeschke, M.G. Burn Infections and Sepsis: Challenges and Future Prospects of Antibacterial Therapy. *Antibiotics* **2026**, *15*, 383. [CrossRef] [PubMed]
6. Cooper, R.A.; Jenkins, L.; Henriques, A.F.M.; Duggan, R.S.; Burton, N.F. Absence of Bacterial Resistance to Medical-Grade Manuka Honey. *Eur. J. Clin. Microbiol. Infect. Dis.* **2010**, *29*, 1237–1241. [CrossRef] [PubMed]
7. Bischofberger, A.M.; Pfrunder Cardozo, K.R.; Baumgartner, M.; Hall, A.R. Evolution of Honey Resistance in Experimental Populations of Bacteria Depends on the Type of Honey and Has No Major Side Effects for Antibiotic Susceptibility. *Evol. Appl.* **2021**, *14*, 1314–1327. [CrossRef] [PubMed]
8. Silva, K.J.S.; Abreu, A.C.S.; De Souza, S.G.B.; De Oliveira, J.T.L.B.; De Sousa, C.L.; Vasconcelos, A.A.; Azevedo, M.M.R.; De Souza, J.; Da Silva, S.K.R.; Gul, K.; et al. Study of Brazilian Amazon Honeybees' (*Melipona scutellaris* and *Apis mellifera*) Properties in Healing Infected Skin Wounds in Wistar Rats. *Curr. Biotechnol.* **2025**, *14*, 16–28. [CrossRef]
9. Ávila, S.; Hornung, P.S.; Teixeira, G.L.; Malunga, L.N.; Apea-Bah, F.B.; Beux, M.R.; Beta, T.; Ribani, R.H. Bioactive Compounds and Biological Properties of Brazilian Stingless Bee Honey Have a Strong Relationship with the Pollen Floral Origin. *Food Res. Int.* **2019**, *123*, 1–10. [CrossRef] [PubMed]
10. Tyers, M.; Wright, G.D. Drug Combinations: A Strategy to Extend the Life of Antibiotics in the 21st Century. *Nat. Rev. Microbiol.* **2019**, *17*, 141–155. [CrossRef] [PubMed]
11. Hadagali, M.D.; Chua, L.S. The Anti-Inflammatory and Wound Healing Properties of Honey. *Eur. Food Res. Technol.* **2014**, *239*, 1003–1014. [CrossRef]
12. Fahim, M.; Shahzaib, A.; Nishat, N.; Jahan, A.; Bhat, T.A.; Inam, A. Green Synthesis of Silver Nanoparticles: A Comprehensive Review of Methods, Influencing Factors, and Applications. *JCIS Open* **2024**, *16*, 100125. [CrossRef]
13. Wypij, M.; Jędrzejewski, T.; Trzcińska-Wencel, J.; Ostrowski, M.; Rai, M.; Golińska, P. Green Synthesized Silver Nanoparticles: Antibacterial and Anticancer Activities, Biocompatibility, and Analyses of Surface-Attached Proteins. *Front. Microbiol.* **2021**, *12*, 632505. [CrossRef] [PubMed]
14. Guilger-Casagrande, M.; Germano-Costa, T.; Bilesky-José, N.; Pasquoto-Stigliani, T.; Carvalho, L.; Fraceto, L.F.; De Lima, R. Influence of the Capping of Biogenic Silver Nanoparticles on Their Toxicity and Mechanism of Action towards *Sclerotinia sclerotiorum*. *J. Nanobiotechnol* **2021**, *19*, 53. [CrossRef] [PubMed]
15. Muñoz, M.; Del Sol, M.; Vásquez, B. Antibacterial and Wound-Healing Action of Ulmo Honey (*Eucryphia cordifolia*) of Differing Degrees of Purity. *Front. Vet. Sci.* **2023**, *10*, 1172025. [CrossRef] [PubMed]
16. Zainuddin, A.N.Z.; Mustakim, N.N.; Rosemanzailani, F.A.; Fadilah, N.I.M.; Maarof, M.; Fauzi, M.B. A Comprehensive Review of Honey-Containing Hydrogel for Wound Healing Applications. *Gels* **2025**, *11*, 194. [CrossRef] [PubMed]

17. Vijapur, L.S.; Shalavadi, M.; Desai, A.R.; Hiremath, J.N.; Gudigennavar, A.S.; Shidramshettar, S.L.; Hiremath, S.R.; Peram, M.R.; Kittur, B.S. Wound Healing Potential of Green Synthesized Silver Nanoparticles of *Glycyrrhiza glabra* Linn Root Extract: A Preclinical Study. *J. Trace Elem. Miner.* **2025**, *11*, 100214. [CrossRef]
18. Philip, D. Honey Mediated Green Synthesis of Silver Nanoparticles. *Spectrochim. Acta Part A Mol. Biomol. Spectrosc.* **2010**, *75*, 1078–1081. [CrossRef] [PubMed]
19. Abusalim, G.S.; Alissa, M. Honey-Biosynthesized Silver Nanoparticles against Vancomycin-Resistant Enterococci: Integrated Antibacterial, Antibiofilm, Mechanistic and Preliminary Safety Evaluation. *Sci. Rep.* **2026**, *16*, 24735. [CrossRef] [PubMed]
20. Bahari, N.; Hashim, N.; Abdan, K.; Akim, A.M.; Maringgal, B.; Al-Shdifat, L. Green-Synthesised Silver and Zinc Oxide Nanoparticles from Stingless Bee Honey: Morphological Characterisation, Antimicrobial Action, and Cytotoxic Assessment. *Chemosphere* **2025**, *370*, 143961. [CrossRef] [PubMed]
21. Abreu, A.C.S.; Júnior, J.S.A.; Moraes, W.P.; Silva, H.N.P.; Fernandes, G.S.T.; Souza, J.; Azevedo, M.M.R.; Lima, A.K.O.; Silveira, T.S.; Gusmão, J.G.V.; et al. Synthesis of Silver Nanoparticles Assisted by Amazonian Stingless Honeybee from *Melipona compressipes manaosensis* and Application in Tissue Repair of Infected Wounds in Wistar Rats. *Regen. Eng. Transl. Med.* **2026**, *12*, 315–331. [CrossRef]
22. Santos, A.C.C.; Batista, G.C.; Cerqueira, R.C.; Lisboa, M.G.; Correa, J.L.; Rodrigues, T.S.; Da Silva, M.N.T.; Bittar, V.P.; Malta, S.M.; Dos Santos, N.C.L.; et al. Green Synthesis of Silver Nanoparticle Using Pollen Extract from *Tetragonisca angustula* a Stingless Bee. *Discov. Nano* **2024**, *19*, 92. [CrossRef] [PubMed]
23. Santos, A.C.C.; Corrêa, J.L.; Cerqueira, R.C.; Batista, G.C.; Rodrigues, T.S.; Bernardes, L.M.M.; Duarte, R.M.; Espindola, F.S.; Bastos, L.M.; Martins, M.M.; et al. Microbial Synthesis of Silver Nanoparticles Using Bacterial Supernatants from Brazilian Stingless Bees with Antimicrobial Activity. *Sci. Rep.* **2026**, *16*, 8512. [CrossRef] [PubMed]
24. Guruvu, N.; Narapogu, V.; Lalitha, D.; Bandaru, B.; Goothy, S.; Rao, D. Synergistic Antimicrobial Activity of Honey Combined with Silver Nanoparticles Topically Applied in Experimentally Infected Wounds in Wistar Albino Rats. *Natl. J. Physiol. Pharm. Pharmacol.* **2022**, *12*, 1–5. [CrossRef]
25. Senanayake, K.; Kumbukgolla, W.W.; Jayaweera, J.A.A.S. The Synergy between Sri Lankan Bee Honey and Silver Nanoparticles on Pathogenic Bacteria. *Microbe* **2025**, *7*, 100373. [CrossRef]
26. Taherpour, A.; Mirzavi, F.; Shafaei, E.; Zarban, A.; Shakibaie, M. Combined Effects of Honey and Silver Nanoparticles on Wound Healing in Human Dermal Fibroblast Cells. *BMC Complement. Med. Ther.* **2025**, *25*, 446. [CrossRef] [PubMed]
27. Tiang, E.R.; Han, L.; Hu, F. Physicochemical Characteristics, Antioxidant Capacity, and Antimicrobial Activity of Stingless Bee Honey from Malaysia: *Heterotrigona itama*, *Lophotrigona canifrons*, and *Tetrigona binghami*. *Foods* **2025**, *14*, 995. [CrossRef] [PubMed]
28. Fernandes, K.E.; Levina, A.; Cokcetin, N.N.; Haley, D.; Li, J.; Brooks, P.; Gloag, R.; Carter, D.A. Strong Antimicrobial Activity and Unique Physicochemical Characteristics in Honey from Australian Stingless Bees *Tetragonula carbonaria*, *Tetragonula hockingsi*, and *Austroplebeia australis*. *Appl. Environ. Microbiol.* **2025**, *91*, e02523-24. [CrossRef] [PubMed]
29. Mduda, C.A.; Muruke, M.H.; Joseph, C.O.; Hussein, J.M. Antioxidant and Antibacterial Properties of Stingless Bee (*Meliponula* spp.) Honey from the Northern Highlands of Tanzania, in Comparison with *Apis mellifera* Honey. *Food Humanit.* **2024**, *2*, 100310. [CrossRef]
30. Albaridi, N.A. Antibacterial Potency of Honey. *Int. J. Microbiol.* **2019**, *2019*, 1–10. [CrossRef] [PubMed]
31. Brudzynski, K.; Abubaker, K.; Laurent, M.; Castle, A. Re-Examining the Role of Hydrogen Peroxide in Bacteriostatic and Bactericidal Activities of Honey. *Front. Microbiol.* **2011**, *2*, 213. [CrossRef] [PubMed]
32. Nishio, E.K.; Ribeiro, J.M.; Oliveira, A.G.; Andrade, C.G.T.J.; Proni, E.A.; Kobayashi, R.K.T.; Nakazato, G. Antibacterial Synergic Effect of Honey from Two Stingless Bees: *Scaptotrigona bipunctata* Lepeletier, 1836, and *S. postica* Latreille, 1807. *Sci. Rep.* **2016**, *6*, 21641. [CrossRef] [PubMed]
33. Nolan, V.C.; Harrison, J.; Cox, J.A.G. Dissecting the Antimicrobial Composition of Honey. *Antibiotics* **2019**, *8*, 251. [CrossRef] [PubMed]
34. Veiko, A.G.; Olchowik-Grabarek, E.; Sekowski, S.; Roszkowska, A.; Lapshina, E.A.; Dobrzynska, I.; Zamaraeva, M.; Zavodnik, I.B. Antimicrobial Activity of Quercetin, Naringenin and Catechin: Flavonoids Inhibit *Staphylococcus aureus*-Induced Hemolysis and Modify Membranes of Bacteria and Erythrocytes. *Molecules* **2023**, *28*, 1252. [CrossRef] [PubMed]
35. Lou, Z.; Wang, H.; Rao, S.; Sun, J.; Ma, C.; Li, J. *p*-Coumaric Acid Kills Bacteria through Dual Damage Mechanisms. *Food Control* **2012**, *25*, 550–554. [CrossRef]
36. Plaper, A.; Golob, M.; Hafner, I.; Oblak, M.; Šolmajer, T.; Jerala, R. Characterization of Quercetin Binding Site on DNA Gyrase. *Biochem. Biophys. Res. Commun.* **2003**, *306*, 530–536. [CrossRef] [PubMed]
37. Borges, A.; Ferreira, C.; Saavedra, M.J.; Simões, M. Antibacterial Activity and Mode of Action of Ferulic and Gallic Acids Against Pathogenic Bacteria. *Microb. Drug Resist.* **2013**, *19*, 256–265. [CrossRef] [PubMed]
38. Shi, C.; Sun, Y.; Zheng, Z.; Zhang, X.; Song, K.; Jia, Z.; Chen, Y.; Yang, M.; Liu, X.; Dong, R.; et al. Antimicrobial Activity of Syringic Acid against *Cronobacter sakazakii* and Its Effect on Cell Membrane. *Food Chem.* **2016**, *197*, 100–106. [CrossRef] [PubMed]

39. Biluca, F.C.; De Gois, J.S.; Schulz, M.; Braghini, F.; Gonzaga, L.V.; Maltez, H.F.; Rodrigues, E.; Vitali, L.; Micke, G.A.; Borges, D.L.G.; et al. Phenolic Compounds, Antioxidant Capacity and Bioaccessibility of Minerals of Stingless Bee Honey (Meliponinae). *J. Food Compos. Anal.* **2017**, *63*, 89–97. [CrossRef]
40. Biluca, F.C.; Da Silva, B.; Caon, T.; Mohr, E.T.B.; Vieira, G.N.; Gonzaga, L.V.; Vitali, L.; Micke, G.; Fett, R.; Dalmarco, E.M.; et al. Investigation of Phenolic Compounds, Antioxidant and Anti-Inflammatory Activities in Stingless Bee Honey (Meliponinae). *Food Res. Int.* **2020**, *129*, 108756. [CrossRef] [PubMed]
41. Rozman, A.S.; Hashim, N.; Maringgal, B.; Abdan, K. A Comprehensive Review of Stingless Bee Products: Phytochemical Composition and Beneficial Properties of Honey, Propolis, and Pollen. *Appl. Sci.* **2022**, *12*, 6370. [CrossRef]
42. Nikaido, H. Molecular Basis of Bacterial Outer Membrane Permeability Revisited. *Microbiol. Mol. Biol. Rev.* **2003**, *67*, 593–656. [CrossRef] [PubMed]
43. Dakal, T.C.; Kumar, A.; Majumdar, R.S.; Yadav, V. Mechanistic Basis of Antimicrobial Actions of Silver Nanoparticles. *Front. Microbiol.* **2016**, *7*, 1831. [CrossRef] [PubMed]
44. Dong, F.; Zhou, Y. Differential Transformation and Antibacterial Effects of Silver Nanoparticles in Aerobic and Anaerobic Environment. *Nanotoxicology* **2019**, *13*, 339–353. [CrossRef] [PubMed]
45. Hu, R.; Deng, L.; Hao, X.; Chen, J.; Zhou, X.; Sahai, N. Direct, Broad-Spectrum Antimicrobial Activity of Ag+-Doped Hydroxyapatite against Fastidious Anaerobic Periodontal and Aerobic Dental Bacteria. *Materials* **2024**, *17*, 4688. [CrossRef] [PubMed]
46. Vergalli, J.; Bodrenko, I.V.; Masi, M.; Moynié, L.; Acosta-Gutiérrez, S.; Naismith, J.H.; Davin-Regli, A.; Ceccarelli, M.; Van Den Berg, B.; Winterhalter, M.; et al. Porins and Small-Molecule Translocation across the Outer Membrane of Gram-Negative Bacteria. *Nat. Rev. Microbiol.* **2020**, *18*, 164–176. [CrossRef] [PubMed]
47. Durán, N.; Durán, M.; De Jesus, M.B.; Seabra, A.B.; Fávaro, W.J.; Nakazato, G. Silver Nanoparticles: A New View on Mechanistic Aspects on Antimicrobial Activity. *Nanomed. Nanotechnol. Biol. Med.* **2016**, *12*, 789–799. [CrossRef] [PubMed]
48. Ferreyra Maillard, A.P.V.; Dalmasso, P.R.; López De Mishima, B.A.; Hollmann, A. Interaction of Green Silver Nanoparticles with Model Membranes: Possible Role in the Antibacterial Activity. *Colloids Surf. B Biointerfaces* **2018**, *171*, 320–326. [CrossRef] [PubMed]
49. Alkawareek, M.Y.; Bahlool, A.; Abulateefeh, S.R.; Alkilany, A.M. Synergistic Antibacterial Activity of Silver Nanoparticles and Hydrogen Peroxide. *PLoS ONE* **2019**, *14*, e0220575. [CrossRef] [PubMed]
50. Campos, F.M.; Couto, J.A.; Figueiredo, A.R.; Tóth, I.V.; Rangel, A.O.S.S.; Hogg, T.A. Cell Membrane Damage Induced by Phenolic Acids on Wine Lactic Acid Bacteria. *Int. J. Food Microbiol.* **2009**, *135*, 144–151. [CrossRef] [PubMed]
51. Vazquez-Muñoz, R.; Meza-Villezcas, A.; Fournier, P.G.J.; Soria-Castro, E.; Juarez-Moreno, K.; Gallego-Hernández, A.L.; Bogdanchikova, N.; Vazquez-Duhalt, R.; Huerta-Saquero, A. Enhancement of Antibiotics Antimicrobial Activity Due to the Silver Nanoparticles Impact on the Cell Membrane. *PLoS ONE* **2019**, *14*, e0224904. [CrossRef] [PubMed]
52. Odds, F.C. Synergy, Antagonism, and What the Chequerboard Puts between Them. *J. Antimicrob. Chemother.* **2003**, *52*, 1. [CrossRef] [PubMed]
53. Shettigar, K.; Murali, T.S. Virulence Factors and Clonal Diversity of *Staphylococcus aureus* in Colonization and Wound Infection with Emphasis on Diabetic Foot Infection. *Eur. J. Clin. Microbiol. Infect. Dis.* **2020**, *39*, 2235–2246. [CrossRef] [PubMed]
54. Norbury, W.; Herndon, D.N.; Tanksley, J.; Jeschke, M.G.; Finnerty, C.C.; on Behalf of the Scientific Study Committee of the Surgical Infection Society. Infection in Burns. *Surg. Infect.* **2016**, *17*, 250–255. [CrossRef] [PubMed]
55. David, A.; Tahrioui, A.; Tareau, A.-S.; Forge, A.; Gonzalez, M.; Bouffartigues, E.; Lesouhaitier, O.; Chevalier, S. *Pseudomonas aeruginosa* Biofilm Lifecycle: Involvement of Mechanical Constraints and Timeline of Matrix Production. *Antibiotics* **2024**, *13*, 688. [CrossRef] [PubMed]
56. Scandorieiro, S.; Rodrigues, B.C.D.; Nishio, E.K.; Panagio, L.A.; De Oliveira, A.G.; Durán, N.; Nakazato, G.; Kobayashi, R.K.T. Biogenic Silver Nanoparticles Strategically Combined With *Origanum vulgare* Derivatives: Antibacterial Mechanism of Action and Effect on Multidrug-Resistant Strains. *Front. Microbiol.* **2022**, *13*, 842600. [CrossRef] [PubMed]
57. Kim, S.-H.; Lee, H.-S.; Ryu, D.-S.; Choi, S.-J.; Lee, D.-S. Antibacterial Activity of Silver-Nanoparticles Against *Staphylococcus aureus* and *Escherichia coli*. *Korean J. Microbiol. Biotechnol.* **2011**, *39*, 77–85.
58. Henriques, A.F.; Jenkins, R.E.; Burton, N.F.; Cooper, R.A. The Intracellular Effects of Manuka Honey on *Staphylococcus aureus*. *Eur. J. Clin. Microbiol. Infect. Dis.* **2010**, *29*, 45–50. [CrossRef] [PubMed]
59. Shrestha, S.; Wang, B.; Dutta, P.K. Commercial Silver-Based Dressings: In Vitro and Clinical Studies in Treatment of Chronic and Burn Wounds. *Antibiotics* **2024**, *13*, 910. [CrossRef] [PubMed]
60. Magiorakos, A.-P.; Srinivasan, A.; Carey, R.B.; Carmeli, Y.; Falagas, M.E.; Giske, C.G.; Harbarth, S.; Hindler, J.F.; Kahlmeter, G.; Olsson-Liljequist, B.; et al. Multidrug-Resistant, Extensively Drug-Resistant and Pandrug-Resistant Bacteria: An International Expert Proposal for Interim Standard Definitions for Acquired Resistance. *Clin. Microbiol. Infect.* **2012**, *18*, 268–281. [CrossRef] [PubMed]

61. Okino, G.A.K.; Nakazato, G.; Kobayashi, R.K.T.; Panagio, L.A.; de Campos, A.C.L.P.; Chue, M.G.; Lonni, A.A.S.G. Processo de Produção de Nanopartículas Biogênicas de Prata, Nanopartículas Biogênicas de Prata e Usos Das Nanopartículas Biogênicas de Prata. BR102021016375B1, 8 November 2022.
62. Spoladori, L.F.D.A.; Andriani, G.M.; Castro, I.M.D.; Suzukawa, H.T.; Gimenes, A.C.R.; Bartolomeu-Gonçalves, G.; Ishida, K.; Nakazato, G.; Pinge-Filho, P.; Machado, R.R.B.; et al. Synergistic Antifungal Interaction between *Pseudomonas aeruginosa* LV Strain Metabolites and Biogenic Silver Nanoparticles against *Candida auris*. *Antibiotics* **2023**, *12*, 861. [CrossRef] [PubMed]
63. Kashiwaqui, N.Y.; Suzukawa, H.T.; Bigotto, B.G.; Thomé, M.L.F.L.; Lazarin Bidoia, D.; Yamada-Ogatta, S.F.; Almeida, R.S.C.D.; Garcia Lonni, A.A.S.; Sumini, M.; Kobayashi, R.K.T.; et al. Development and Characterization of a Silver Nanoparticle-Based Hydrogel Containing Hyaluronic Acid and Allantoin for Antibacterial Burn Treatment. *Pharmaceutics* **2026**, *18*, 724. [CrossRef] [PubMed]
64. *CLSI M07*; Methods for Dilution Antimicrobial Susceptibility Tests for Bacteria That Grow Aerobically. Clinical and Laboratory Standards Institute: Wayne, PA, USA, 2018.
65. *CLSI M26-A*; Methods for Determining Bactericidal Activity of Antimicrobial Agents. National Committee for Clinical Laboratory Standards: Wayne, PA, USA, 1999.
66. Domínguez, A.V.; Panadero, I.M.; Smani, Y. In Vitro and in Vivo Evaluation of Two Combined β-Lactamase Inhibitors against Carbapenem-Resistant *Acinetobacter baumannii*. *Eur. J. Clin. Microbiol. Infect. Dis.* **2023**, *42*, 1317–1325. [CrossRef] [PubMed]
67. Santos, M.H.D.M.; Endo, T.H.; Scandorieiro, S.; Pavanelli, W.R.; Kobayashi, R.K.T.; Nakazato, G. Silver Nanoparticle–Antibiotic Combinations: A Strategy to Overcome Bacterial Resistance in *Escherichia coli*, *Salmonella* Enteritidis and *Staphylococcus aureus*. *Antibiotics* **2025**, *14*, 960. [CrossRef] [PubMed]
68. European Committee for Antimicrobial Susceptibility Testing (EUCAST) of the European Society of Clinical Microbiology and Infectious Diseases (ESCMID). Terminology Relating to Methods for the Determination of Susceptibility of Bacteria to Antimicrobial Agents. *Clin. Microbiol. Infect.* **2000**, *6*, 503–508. [CrossRef] [PubMed]
69. Scandorieiro, S.; De Camargo, L.C.; Lancheros, C.A.C.; Yamada-Ogatta, S.F.; Nakamura, C.V.; De Oliveira, A.G.; Andrade, C.G.T.J.; Duran, N.; Nakazato, G.; Kobayashi, R.K.T. Synergistic and Additive Effect of Oregano Essential Oil and Biological Silver Nanoparticles against Multidrug-Resistant Bacterial Strains. *Front. Microbiol.* **2016**, *7*, 760. [CrossRef] [PubMed]
70. *10993-5:2009*; Biological Evaluation of Medical Devices—Part 5: Tests for In Vitro Cytotoxicity. International Organization for Standardization: Geneva, Switzerland, 2009.
71. Famuyide, I.M.; Aro, A.O.; Fasina, F.O.; Eloff, J.N.; McGaw, L.J. Antibacterial and Antibiofilm Activity of Acetone Leaf Extracts of Nine Under-Investigated South African *Eugenia* and *Syzygium* (Myrtaceae) Species and Their Selectivity Indices. *BMC Complement. Altern. Med.* **2019**, *19*, 141. [CrossRef] [PubMed]

Disclaimer/Publisher's Note: The statements, opinions and data contained in all publications are solely those of the individual author(s) and contributor(s) and not of MDPI and/or the editor(s). MDPI and/or the editor(s) disclaim responsibility for any injury to people or property resulting from any ideas, methods, instructions or products referred to in the content.